Letters

Minimum-Loss Short Reflectors on 128° $LiNbO_3$

Saku Lehtonen, Victor P. Plessky, *Senior Member, IEEE*, Natacha Béreux, and Martti M. Salomaa, *Member, IEEE*

***Abstract*—We consider the interaction of surface acoustic waves (SAWs) with short electrode gratings encompassing only few electrodes on 128° lithium niobate ($LiNbO_3$). The qualifications of the reflectors are evaluated by comparing the part of incident SAW energy scattered by the structure into the bulk to the energy reflected back as a SAW.**

I. Introduction

We report results complementary to those of [1] obtained from the rigorous simulation of the operation of surface acoustic wave (SAW) reflectors comprising one to three electrodes on the well-known 128° YX-cut lithium niobate ($LiNbO_3$) [2]. We evaluate the feasibility of such short reflectors by comparing the energy scattered by the structure into the bulk to that reflected back as a SAW. The magnitude of the normalized reflection coefficient as well as quantitative estimates of the attenuation due to the scattering into the bulk were reported in [1].

II. Research Methods

The gratings ($N_{el} = 1 \ldots 3$) studied operate either at the fundamental harmonic frequency or at the second harmonic. In the former case, the center-to-center distance between the adjacent electrodes d is close to half the SAW wavelength $\lambda_0/2$, and for second-harmonic operation, $d \propto \lambda_0$. The gratings are either grounded or open-circuited.

The test structure used in the numerical experiment is described in [1]. Similar to the test setup in [3], it comprises a fundamental-mode input transducer ($N_{el} = 21$, electric port 1), two identical split-finger receiving transducers ($N_{el} = 6$, electric ports 2 and 3), and the grating studied, centered between the receiving transducers. The purpose of the centering is to render the SAW propagation paths of the waves reflected from and transmitted through the grating equal. Consequently, the propagation times of the corresponding signals are equal. A test structure with the grating absent is used as a reference. The reasons for choosing the numbers of fingers in the different elements of the test structure are discussed in [1].

The characteristics of the grating were addressed through numerical simulations. A rigorous simulation tool [4], [5] based on the application of Green's function formalism, the finite-element and boundary-element methods (FEM, BEM) was used for generating the electrical response of the test structure setup, a frequency-dependent three-port admittance matrix. The propagation loss and the resistivity of the electrodes were excluded.

The elements of the admittance matrix, or the Y parameters, are proportional to the electric currents generated in the transducers. The currents present in the receiving transducers due to the input voltage, characterized by $Y_{21}(f)$ and $Y_{31}(f)$, are of particular interest because they are further proportional to the amplitudes of the SAWs incident on the receiving transducers. However, the Y parameters characterize the aggregate of all acoustic-wave contributions incident on the transducer. Application of the time gating procedure described in [1] allows one to separate from $Y_{21}(f)$ and $Y_{31}(f)$ the partial signals of interest. For example, the signal attributed to the SAW transmitted from the input transducer, reflected once from the grating and registered at port 2, $Y^r_{21}(f)$, corresponds to the reflected wave. Similarly, the partial signal corresponding to the direct transmission from the input transducer to the receiving transducer at port 3, $Y^d_{31}(f)$, and the corresponding reference obtained for the reference test structure with the grating absent, $Y^{d,ref}_{31}(f)$, can be extracted. Because the propagation attenuation of the SAW and the resistivity of the electrodes are excluded from the simulations, energy consideration of these three contributions then yields a means for the evaluation of losses due to the scattering into the bulk:

$$E_{sc}(f) = |Y^{d,\,ref}_{31}(f)|^2 - |Y^d_{31}(f)|^2 - |Y^r_{21}(f)|^2. \quad (1)$$

Because the applicability of short gratings as reflecting elements is considered, one preferably needs to simultaneously attain a high, or at least a moderate, value for the reflectivity and as small scattering losses as possible. These criteria can be illustrated by considering the ratio of the energies scattered and reflected:

$$\frac{E_{sc}(f)}{E_r(f)} = \frac{|Y^{d,\,ref}_{31}(f)|^2 - |Y^d_{31}(f)|^2 - |Y^r_{21}(f)|^2}{|Y^r_{21}(f)|^2}. \quad (2)$$

The ratio E_{sc}/E_r is frequency dependent. Here it is evaluated as a mean value within the -3 dB frequency band with respect to the maximum of the reference response $|Y^{d,\,ref}_{31}|$ [1].

The rigorous FEM/BEM simulator [4], [5] was applied to evaluate the feasibility of short reflectors on 128° YX-

Manuscript received March 9, 2004; accepted May 25, 2004.

S. Lehtonen and M. M. Salomaa are with the Materials Physics Laboratory, Helsinki University of Technology, FIN-02015 HUT, Finland (e-mail: saku@focus.hut.fi).

V. P. Plessky is with GVR Trade SA, CH-2022 Bevaix, Switzerland.

N. Béreux is with Centre de Mathématiques Appliquées (CMAP), Unité Mixte de Recherche 7641, Centre National de la Recherche Scientifique/Ecole Polytechnique, 91228 Palaiseau Cedex, France.

cut $LiNbO_3$. The reflectors are either grounded or open-circuited. The materials parameters by Kovacs *et al.* [6] were used, and the aluminum electrodes were assumed rectangular and isotropic. The results are presented as a function of the metallization ratio a/p (for the second harmonic grating, $a/p = a/\lambda_0$) and the relative electrode thickness h/λ_0.

III. Results

The ratio of the energy scattered into the bulk and the energy reflected is shown for a single-electrode reflector in Fig. 1 and for reflectors with two and three floating electrodes in Fig. 2. For the single-electrode geometry, the energy scattered is higher than that reflected. Comparing Figs. 1(a) and (b), one may verify that, for the practical metallization ratios $a/p = 0.40 \ldots 0.60$ and thicknesses $h/\lambda_0 = 5\% \ldots 8\%$, the energy ratio E_{sc}/E_r for a floating electrode is 40% to 80%. If the reflecting electrode is terminated to ground, the minimum occurs approximately for $a/p = 0.80$, see Fig. l(c) for second-harmonic operation ($a/\lambda_0 = 0.40$). It is deduced that, for single electrodes, floating or wide grounded electrodes are to be favored when energy losses are to be minimized. The minimum of E_{sc}/E_r in Fig. 1(c) originates from the fact that the reflection coefficient decreases to zero for both large and small values of a/p while scattering into the bulk remains significant.

The ratio E_{sc}/E_r is reduced with the inclusion of electrodes in the grating, compare Figs. 1(b), 2(a), and 2(b) for the reflectors with floating electrodes. This is expected as the total reflectivity of a grating increases with its length. The end effects (i.e., scattering from the ends of a periodic grating), are expected to exhibit only a weak dependence on the grating length. Fig. 3 shows the energy scattered into the bulk normalized to the reference for the electrode thickness $h/\lambda_0 = 5\%$. The results obtained agree well with the experimental value recently published for losses in short gratings [7]. It is noted that, for fundamental-mode reflectors with floating electrodes, the inclusion of the second electrode increases the scattering loss by approximately 50%. For a three-electrode, open-circuited grating, the scattering loss is even slightly lower than that of a two-electrode grating. This is assumed to originate from the fact that, in certain directions, the contributions of bulk waves scattered into the bulk have opposite phases and cancel out. For a single, fundamental-mode grounded electrode, the scattering loss is visibly higher than that of a floating electrode. For a single, grounded electrode operating at the second harmonic, the scattering loss is further increased. Note that, for this curve, contrary to other curves in Fig. 3, the period is taken to be $p_{2^{\text{nd}}\ \text{harmonic}} = \lambda_0$. Thus, for a given metallization ratio, the second-harmonic electrode has twice the width of a fundamental-mode electrode. For a single grounded electrode, the apparent difference between the second-harmonic and fundamental-mode cases is a consequence of normalization. For exam-

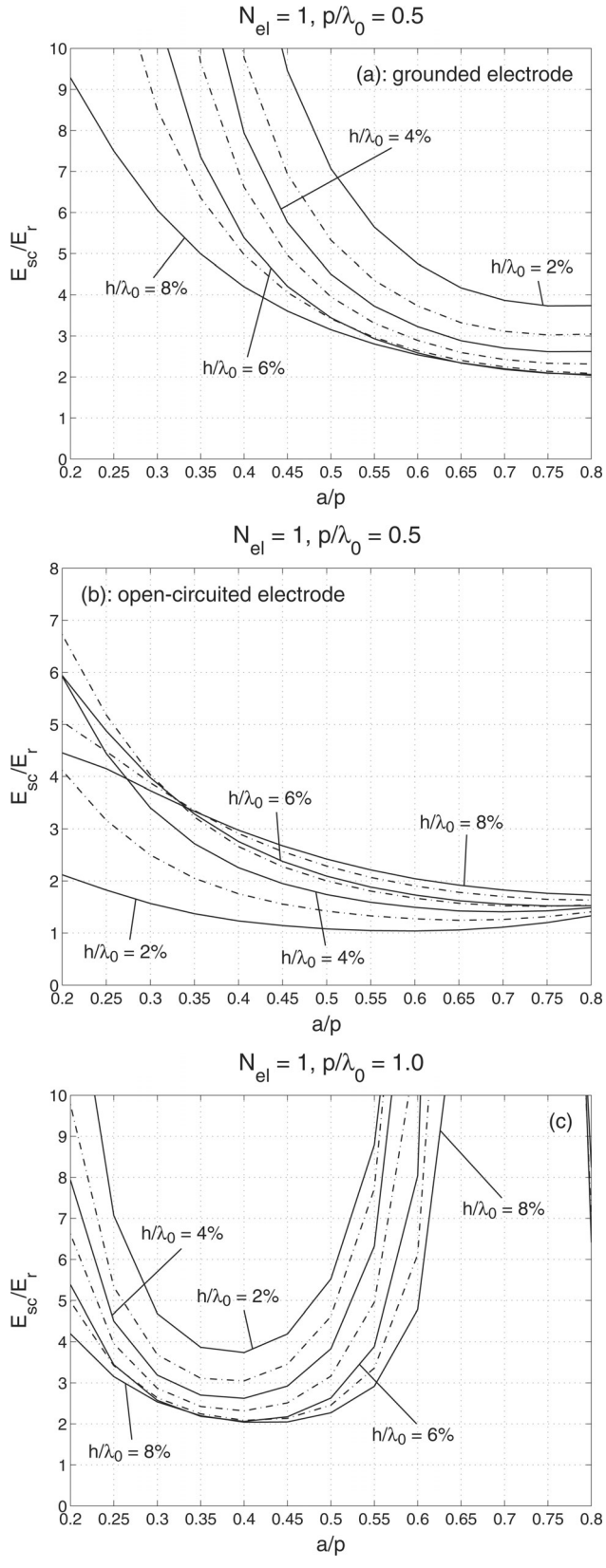

Fig. 1. Ratio of the energy scattered into the bulk and the energy reflected for a single electrode finger as a function of the aluminum thickness h/λ_0 and metallization ratio a/p. (a) Fundamental mode of operation ($p = \lambda_0/2$), grounded electrode. (b) Fundamental mode of operation ($p = \lambda_0/2$), open-circuited electrode. (c) Second-harmonic mode ($p = \lambda_0$), grounded electrode.

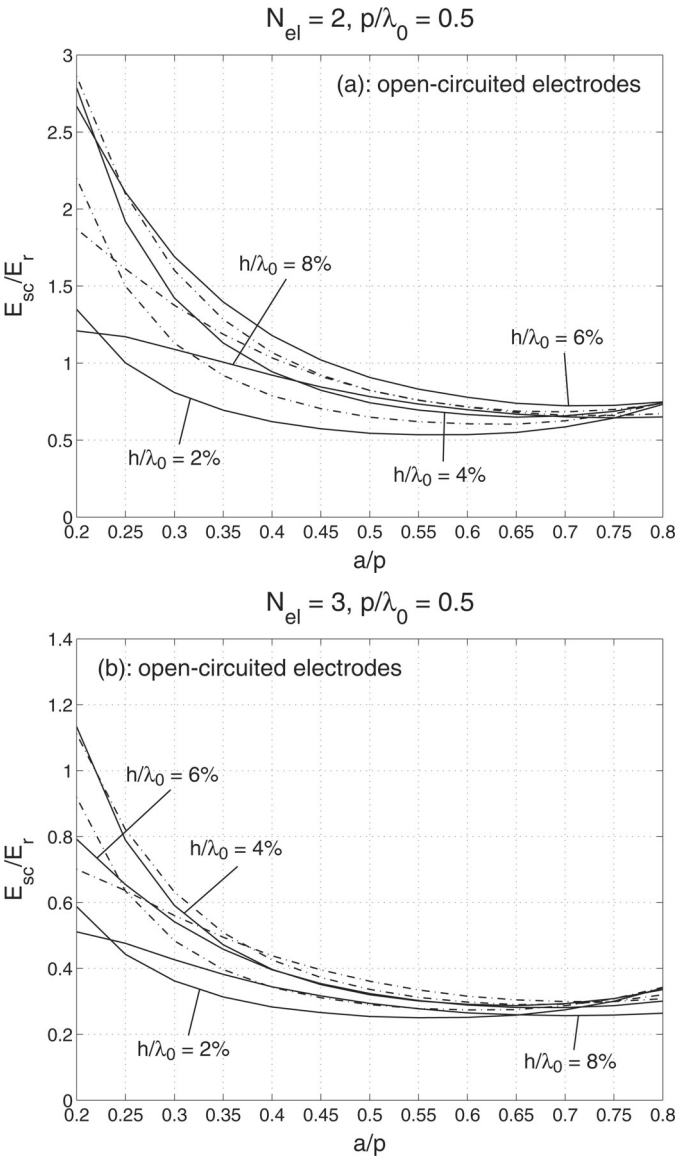

Fig. 2. Ratio of the energy scattered into the bulk and the energy reflected for short fundamental-mode, open-circuited reflectors as a function of the aluminum thickness h/λ_0 and metallization ratio a/p. (a) Grating with two electrodes. (b) Grating with three electrodes.

ple, the point with $a/p = 0.4$ on the curve for the grounded second-harmonic electrode corresponds to $a/p = 0.8$ for the grounded fundamental-mode electrode.

Acknowledgments

The authors are grateful to Clinton Hartmann for enlightening discussions and William Steichen at Temex Microsonics SA for conferring TRANSD[1] at the disposal of HUT for this study. The first author further acknowledges the Academy of Finland for support within the Graduate School in Technical Physics and the Foundation of Technology (Finland) for a scholarship.

[1]TRANSD is a FEM/BEM-based simulator for the analysis of SAWs in finite electrode structures developed by Temex Microsonics SA, Sophia-Antipolis, France, in collaboration with CMAP/Ecole Polytechnique, Paris, France.

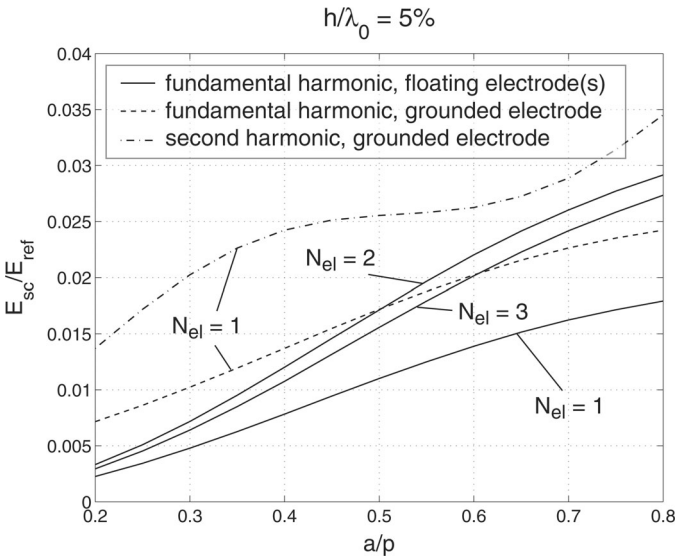

Fig. 3. Ratio of the energy scattered into the bulk and the energy reference as a function of the aluminum thickness h/λ_0 and metallization ratio a/p.

References

[1] S. Lehtonen, V. P. Plessky, and M. M. Salomaa, "Short reflectors operating at the fundamental and second harmonics on 128° LiNbO$_3$," *IEEE Trans. Ultrason., Ferroelect., Freq. Contr.*, vol. 51, pp. 343–351, Mar. 2004.

[2] K. Shibayama, K. Yamanouchi, H. Sato, and T. Meguro, "Optimum cut for rotated Y-cut LiNbO$_3$ crystal used as the substrate of acoustic surface wave filters," *Proc. IEEE*, vol. 64, pp. 595–597, May 1976.

[3] P. Wright, "Modeling and experimental measurements of the reflection properties of SAW metallic gratings," in *Proc. IEEE Ultrason. Symp.*, 1984, pp. 54–63.

[4] J. Ribbe, "On the coupling of integral equations and finite elements/Fourier modes for the simulation of piezoelectric surface acoustic wave components," Ph.D. dissertation, CMAP/Ecole Polytechnique, Paris, France, 2002. (in French)

[5] P. Ventura, J.-M. Hodé, M. Solal, J. Desbois, and J. Ribbe, "Numerical methods for SAW propagation characterization," in *Proc. IEEE Ultrason. Symp.*, 1998, pp. 175–186.

[6] G. Kovacs, M. Anhorn, H. E. Engan, G. Visintini, and C. C. W. Ruppel, "Improved material constants for LiNbO$_3$ and LiTaO$_3$," in *Proc. IEEE Ultrason. Symp.*, 1990, pp. 435–438.

[7] C. S. Hartmann, P. Brown, and J. Bellamy, "Design of global SAW RFID tag devices," in *Proc. Second Int. Symp. on Acoustic Wave Devices for Future Mobile Commun. Syst.*, March 3–5, 2004, pp. 15–19.